International Journal of Engineering Science 121 (2017) 182–193

Contents lists available at ScienceDirect

International Journal of Engineering Science

journal homepage: www.elsevier.com/locate/ijengsci

Redirection of a crack driven by viscous fluid

Monika Perkowska[a], Andrea Piccolroaz[b], Michal Wrobel[c], Gennady Mishuris[d,*]

[a] EnginSoft S.p.A., Via della Stazione 27, frazione Mattarello, 38123 Trento, Italy
[b] Dipartimento di Ingegneria Civile, Ambientale e Meccanica, Universita di Trento, via Mesiano, 77 I-38123 Trento, Italy
[c] Faculty of Energy and Fuels, AGH-University of Science and Technology, 30 Mickiewicza Avenue, 30–059 Krakow, Poland
[d] Department of Mathematics, Aberystwyth University, Ceredigion SY23 3BZ, Wales, United Kingdom

ARTICLE INFO

Article history:
Received 6 September 2017
Revised 22 September 2017
Accepted 25 September 2017
Available online 13 October 2017

Keywords:
Direction of the fracture propagation
Hydraulic fracture
Toughness dominated regime
Viscosity dominated regime

ABSTRACT

As shown by Wrobel, Mishuris, and Piccolroaz (2017), the hydraulically induced tangential traction on fracture walls changes local displacement and stress fields. This resulted in the formulation of a new hydraulic fracture (HF) propagation condition based on the critical value of the energy release rate that accounts for the hydraulically-induced shear stress. Therefore it is clear that the crack direction criteria, which depend on the tip distributions of the stress and strain fields, need to be changed. We analyse the two commonly used criteria, one based on the maximum circumferential stress (MCS) and another - on the minimum strain energy density (MSED). We show that the impact of the hydraulically induced shear stress on the direction of the crack propagation is negligible in the case of large material resistance to fracture, while for small toughness the effect is significant. Moreover, values of the redirection angles, corresponding to the so-called viscosity dominated regime ($K_{IC} \to 0$), depend dramatically on the ratios of the stress intensity factors.

1. Introduction

In the standard approach of Linear Elastic Fracture Mechanics (LEFM), the onset of crack propagation is found by using the energy release rate (ERR) criterion which, in the case of an isotropic elastic material, assumes the form (Rice, 1968):

$$\mathcal{E} = \frac{1+\nu}{E}\left[(1-\nu)\left(K_I^2 + K_{II}^2\right) + K_{III}^2\right] = \mathcal{E}_C \equiv \frac{1-\nu^2}{E}K_{IC}^2, \tag{1}$$

where ν is the Poisson's ratio and E is the Young's modulus, while $\mathcal{E}_C$ and K_{IC} are the experimentally found critical values of ERR and material toughness, respectively. Here K_I, K_{II} and K_{III} are the stress intensity factors pertaining to three basic modes of fracture load. For pure Mode I loading, Eq. (1) transforms into the well known Irwin criterion for crack propagation (Irwin, 1957):

$$K_I = K_{IC}. \tag{2}$$

However, for the mixed mode loading, determination of the direction of the crack growth is of crucial importance.

* Corresponding author.
E-mail address: ggm@aber.ac.uk (G. Mishuris).

https://doi.org/10.1016/j.ijengsci.2017.09.009

The path of possible crack kinks has been extensively studied for many years (see Cotterell & Rice, 1980; Leblond, 1989). Most of the developed theories are based on the information from the Irwin-Williams expansion of the crack tip field (Williams, 1957). Some more advanced criteria utilise additional material parameters related to the underlying physics or other arguments (size of the process zone, size of the possible kink, and so on).

The collection of criteria for kink initiation developed so far to determine the redirection angle in fracture mechanics is extensive. Beginning with the most popular examples: maximum circumferential stress (MCS) (Erdogan & Sih, 1963) and minimum strain energy density (MSED) (Liebowitz & Sih, 1968; Sih, 1974), we can list the maximum strain energy release rate (MSERR) criterion (Hussain, Pu, & Underwood, 1974; Palaniswamy & Knauss, 1972), the local symmetry criterion (Goldstein & Salganik, 1974), the maximum dilatational strain energy density (MDSED) criterion (Theocaris & Andrianopoulos, 1982; Yehia, 1991), the maximum determinant of the stress tensor criterion (Papadopoulos, 1988), the J-criterion (Hellen & Blackburn, 1975), the vector crack tip displacement criterion (Li, 1989), the maximum normal strain criterion (Chang, 1981), the maximum potential energy release rate criterion (Chang, Xu, & Mutoh, 2006), the so-called T-stresses criteria (Williams & Ewing, 1984), and many others. Clearly, the applicability of any specific approach should be justified on a case by case basis, using the strength properties of the materials involved in the study, the loading conditions and available experimental data to validate the selection of criterion. It follows that there is no universal criterion valid for all possible applications. However, in many situations the discrepancies in prediction given by the different criteria are not large and are usually observable only in the deviation from the pure Mode I load (especially for the infinitesimal kinks most of the criteria coincide - see Cotterell & Rice (1980)).

When considering hydraulic fracture (HF), the prediction of the possible crack propagation path becomes even more challenging, as the interaction between the pressurised fluid and the solid and complicated fracture network substantially increases the complexity of the problem (Paluszny & Zimmerman, 2017; Salimzadeh, Paluszny, & Zimmerman, 2017). Moreover, the sets of credible data that could be used to verify theoretical models are limited or inaccessible. There have also been arguments that cast doubt on the applicability of some of the fracture criteria when applied to brittle fracture (Chudnovsky & Gorelik, 1996) and hydraulic fracture (Cherny et al., 2017)).

Wrobel, Mishuris, and Piccolroaz (2017) introduced a modified formulation of the HF problem, accounting for a hydraulically induced tangential (asymmetrical) traction at the crack faces. It was shown that, due to the order of the tip singularity of the hydraulic shear stress, this component of the load cannot be omitted when computing ERR. A new parameter, the hydraulic shear stress intensity factor (K_f), was introduced and proved to play an important role in the HF process. The amended crack propagation criterion, under remote Mode I loading conditions, was formulated as:

$$\mathcal{E} = \frac{1-\nu^2}{E}\left[K_I^2 + 4(1-\nu)K_I K_f\right] = \mathcal{E}_C. \tag{3}$$

This formula includes both, the standard stress intensity factor for Mode I, K_I, and the newly introduced hydraulic shear stress intensity factor, K_f.

Here we analyse how the shear stress induced by moving fluid at the crack faces influences the crack propagation direction in the most general case, when all fracture modes (Mode I, II, III) are taken into account. We focus on two commonly used criteria, Maximum Circumferential Stress (MCS) and Minimum Strain Energy Density (MSED). Presently, we could not find any experimental data to verify the results and therefore determine which of the two criteria is more relevant to hydraulic fracture problems.

The structure of this paper is as follows. In Section 2 a methodology for the computation of the ERR in presence of the hydraulically induced shear stress for mixed mode loading is presented. An asymptotic representation of the stress and strain fields in the vicinity of the fracture tip is given. In Section 3, in a new setting, two criteria are chosen for use in determining the crack propagation angle in the presence of hydraulic tangential traction. Corresponding results are analysed with respect to various crack propagation regimes and values of the Poisson's ratio, and are compared with one another. Finally, we summarise our conclusions in Section 4.

2. Computation of the energy release rate accounting for the shear stress induced by fluid in a mixed mode setting

In the framework of the LEFM, the ERR is computed using the standard J-integral argument (Huber, Nickel, & Kuhn, 1993; Rice, 1968; Richard, Fulland, & Sander, 2004):

$$\mathcal{E}(z) = \lim_{\delta\to 0} J_x^{\delta}(z) = \lim_{\delta\to 0}\int_{\Gamma_\delta}\left\{\frac{1}{2}(\boldsymbol{\sigma}\cdot\boldsymbol{\varepsilon})n_x - \boldsymbol{t}_n\cdot\frac{\partial \boldsymbol{u}}{\partial x}\right\}ds, \tag{4}$$

where Γ_δ is a circular contour of radius δ around the fracture tip, contained in a plane orthogonal to the crack front, $\mathbf{n}$ is the outward normal to the contour Γ_δ, and $\mathbf{t}_n = \boldsymbol{\sigma}\mathbf{n}$ is the traction vector along Γ_δ (see Fig. 1).

The classical fracture criterion (1) is derived directly from formula (4), for an arbitrary mixed mode deformation and smooth crack front. It has been widely adopted in the analysis of hydraulic fracture (Adachi, Siebrits, Peirce, & Desroches, 2007; Bunger, Detournay, & Garagash, 2005; Garagash, 2006; Garagash & Detournay, 1999; Perkowska, Wrobel, & Mishuris, 2016; Wrobel & Mishuris, 2015) on the ad hoc assumption that the hydraulically induced tangential traction is small compared to the net fluid pressure and can thus be neglected. However, Wrobel et al. (2017) showed that the singularity of the hydraulic shear stress is stronger than that of the fluid pressure, and therefore the former cannot be omitted when

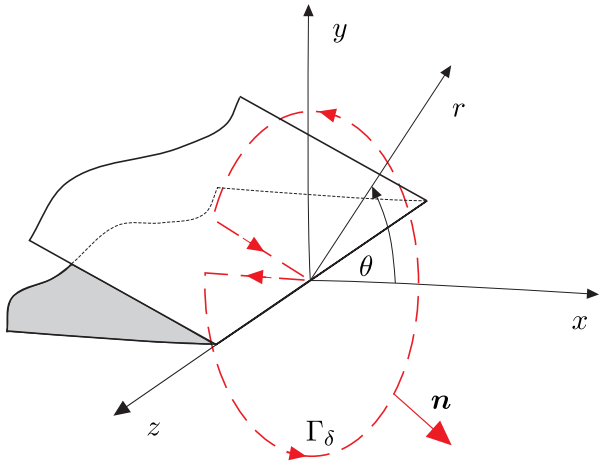

Fig. 1. A planar crack and its local coordinate system.

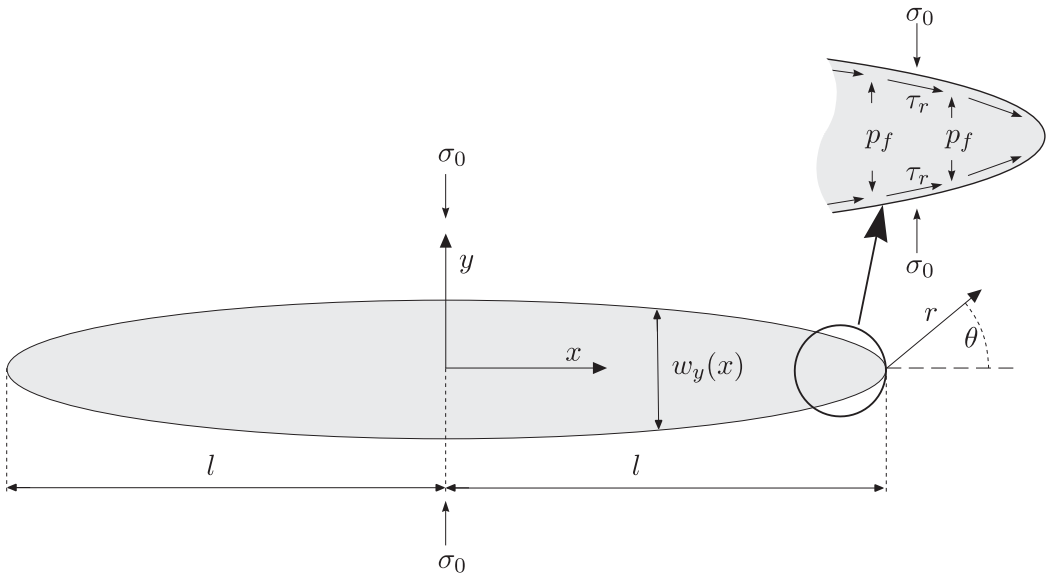

Fig. 2. Sketch of a plane-strain fluid driven fracture.

deriving the integrals in (4). Indeed, in accordance with lubrication theory, the shear stress acting on the crack faces can be computed as (see e.g. Batchelor, 1976):

$$\boldsymbol{\tau}(r,\theta,z)_{|_{\theta=\pm\pi}} = \mp\frac{w_y(r,z)}{2}\nabla_{(r,z)}p(r,z) = \mp\frac{1}{2}w_y\left[\frac{\partial p}{\partial r}\boldsymbol{e}_r + \frac{\partial p}{\partial z}\boldsymbol{e}_z\right], \tag{5}$$

where $w_y(r,z)$ is the width of the crack opening in the direction orthogonal to the crack faces, $p(r,z) = p_f(r,z) - \sigma_0$ is the so-called net fluid pressure in the channel (p_f - fluid pressure, see Fig. 2), and $\boldsymbol{e}_r, \boldsymbol{e}_z$ denote the respective unit vectors.

When considering the tip asymptotics of HF in the so-called toughness dominated regime, which was proved in Wrobel et al. (2017) to be the only permissible type of solution behaviour in the vicinity of the fracture front, we obtain the following estimates for Mode I:

$$w_y(r,z) = w_0(z)\sqrt{r} + O(r), \quad p(r,z) = p_0(z)\log(r) + O(1), \quad r \to 0, \tag{6}$$

and

$$\tau_r(r,\theta,z)_{|_{\theta=\pm\pi}} = \mp\frac{\tau_0(z)}{\sqrt{r}} + O(1), \quad r \to 0, \tag{7}$$

where the multipliers of the leading asymptotic terms are interrelated:

$$\tau_0(z) = \frac{1}{2}p_0(z)w_0(z). \tag{8}$$

In the general case, the complete asymptotic expansions of the displacement and stress fields in the near-tip region ($r \to 0$) are:

$$\mathbf{u}(r,\theta,z) = \sqrt{\frac{r}{2\pi}}\Big[K_I\boldsymbol{\Phi}_I(\theta) + K_{II}\boldsymbol{\Phi}_{II}(\theta) + K_{III}\boldsymbol{\Phi}_{III}(\theta) + K_f\boldsymbol{\Phi}_\tau(\theta)\Big] + O(r\log r), \tag{9}$$

$$\boldsymbol{\sigma}(r,\theta,z) = \frac{1}{\sqrt{2\pi r}}\Big[K_I\boldsymbol{\Psi}_I(\theta) + K_{II}\boldsymbol{\Psi}_{II}(\theta) + K_{III}\boldsymbol{\Psi}_{III}(\theta) + K_f\boldsymbol{\Psi}_\tau(\theta)\Big] + O(\log r), \tag{10}$$

where $\{r, \theta, z\}$ is a local polar coordinate system (see Fig. 1), K_I, K_{II} and K_{III} are the classical stress intensity factors (SIFs) and K_f is the hydraulic shear stress intensity factor (HSSIF) related to the hydraulic shear stress, τ (see (7)). The functions $\boldsymbol{\Phi}_j(\theta)$ and $\boldsymbol{\Psi}_j(\theta)$ define the polar angle dependence and are given in Appendix A. Clearly, all the stress intensity factors in the asymptotic relationships (9) – (10) depend on z, while the vector-functions $\boldsymbol{\Phi}_j$ and $\boldsymbol{\Psi}_j$ are z-independent. Since we will only analyse the local (2D) problem in this paper, we will omit the z variable henceforth.

The above representations were constructed as a superposition of four displacement and stress fields, three of which are related to the classical fracture mechanics loads (Mode I, II and III, where the traction vanishes at the crack surfaces) and the fourth, which is a result of the hydraulic action of fluid via the shear stresses induced on the crack faces.

The asymptotics corresponding respectively to the components of the crack opening, $w_j(r) = u_j(r,+\pi) - u_j(r,-\pi)$, can be expressed by:

$$w_y(r) = \gamma(K_I + K_f)\sqrt{r} + O(r), \quad r \to 0, \tag{11}$$

$$w_x(r) = \gamma K_{II}\sqrt{r} + O(r^{3/2}), \quad w_z(r) = \gamma K_{III}\sqrt{r} + O(r^{3/2}), \quad r \to 0. \tag{12}$$

Comparing these with (6) gives:

$$w_0 = \gamma(K_I + K_f), \quad K_f = \sqrt{\frac{\pi}{2}}\frac{\tau_0}{1-\nu}, \quad \gamma = \frac{8}{\sqrt{2\pi}}\frac{1-\nu^2}{E}. \tag{13}$$

We note that K_I and K_f are not independent. Indeed, combining (8) and (13) we find:

$$K_f = \varpi K_I, \quad \varpi = \frac{p_0}{G - p_0} > 0, \tag{14}$$

where $G = \frac{E}{2(1+\nu)}$ is the shear modulus of the elastic material, and the dimensionless parameter ϖ varies from 0 to ∞. For more details, see Wrobel et al. (2017).

A new formula for the ERR, following from (4) and (9) – (10), can now be given as:

$$\mathcal{E} = \frac{1+\nu}{E}\Big\{(1-\nu)\Big[K_I^2 + K_{II}^2 + 4(1-\nu)K_IK_f\Big] + K_{III}^2\Big\}, \tag{15}$$

which leads to the fracture criterion:

$$K_I^2 + K_{II}^2 + 4(1-\nu)K_IK_f + \frac{1}{1-\nu}K_{III}^2 = K_{IC}^2. \tag{16}$$

We note that conditions (1) and (3) are particular forms of the general formula (16). When the stress intensity factors K_{II} and K_{III} are defined by the external conditions, the expression:

$$K_{IC}^{eff} = \sqrt{K_{IC}^2 - K_{II}^2 - \frac{1}{1-\nu}K_{III}^2} \tag{17}$$

can be considered to be an "effective toughness" for the hydraulic fracture problem under the mixed load.

2.1. Normalisation

In order to facilitate the parametric study, we now introduce the following natural scaling:

$$\hat{K}_I = \frac{K_I}{K_{IC}}, \quad \hat{K}_{II} = \frac{K_{II}}{K_{IC}}, \quad \hat{K}_{III} = \frac{K_{III}}{K_{IC}}, \quad \hat{K}_f = \frac{K_f}{K_{IC}}. \tag{18}$$

The fracture criterion (16) now becomes:

$$\hat{K}_I^2 + \hat{K}_{II}^2 + 4(1-\nu)\hat{K}_I\hat{K}_f + \frac{1}{1-\nu}\hat{K}_{III}^2 = 1. \tag{19}$$

We note that, under such a normalization, the material resistance to brittle fracture described by K_{IC}, is introduced implicitly. On the other hand, identification of the crack propagation regime (viscosity dominated, small and large toughness modes) hinges on this property. Thus, we introduce a dimensionless parameter $\tilde{p}_0 = 2\pi\, p_0(1-\nu^2)/E$, related to material toughness

(compare with equation (71) in the work of Wrobel et al. (2017)), that combines the stress intensity factors $\hat{K}_I$ and $\hat{K}_f$ in the same manner as in Eq. (14):

$$\varpi = \frac{\tilde{p}_0}{\pi(1-\nu) - \tilde{p}_0}, \quad \hat{K}_f = \varpi \hat{K}_I, \quad 0 < \tilde{p}_0 < \pi(1-\nu). \tag{20}$$

The values of the parameter $\tilde{p}_0$ and the stress intensity factors are not independent. As was shown by Wrobel et al. (2017) for the Mode I deformation ($K_{II} = K_{III} = 0$), parameter $\tilde{p}_0$ determines the crack propagation regime ($\tilde{p}_0 \to 0$ corresponds to the toughness dominated one, while $\tilde{p}_0 \to \pi(1-\nu)$ defines the viscosity dominated mode). Taking (17) into account, we conclude that:

$$K_{IC} \cdot \hat{K}_{IC}^{eff} \to \infty \quad \Leftrightarrow \quad \hat{K}_I \to 1 \quad \text{and} \quad \tilde{p}_0 \to 0, \tag{21}$$

and

$$K_{IC} \cdot \hat{K}_{IC}^{eff} \to 0 \quad \Leftrightarrow \quad \hat{K}_I \to 0 \quad \text{and} \quad \tilde{p}_0 \to \pi(1-\nu), \tag{22}$$

where the normalised effective toughness is defined as follows:

$$\hat{K}_{IC}^{eff} = \sqrt{1 - \hat{K}_{II}^2 - \frac{1}{1-\nu}\hat{K}_{III}^2}. \tag{23}$$

The combination of (19) and (20) yields, after rearrangement, a formula for $\hat{K}_I$, provided that $\hat{K}_{II}$, $\hat{K}_{III}$ and $\tilde{p}_0$ are known:

$$\hat{K}_I = \sqrt{\frac{\pi(1-\nu) - \tilde{p}_0}{\pi(1-\nu) + \tilde{p}_0(3-4\nu)}}\, \hat{K}_{IC}^{eff}. \tag{24}$$

After substitution of (20) into (24), and some algebra, we obtain a relation for $\hat{K}_f$:

$$\hat{K}_f = \frac{\tilde{p}_0}{\sqrt{\left[\pi(1-\nu) - \tilde{p}_0\right]\left[\pi(1-\nu) + \tilde{p}_0(3-4\nu)\right]}}\, \hat{K}_{IC}^{eff}. \tag{25}$$

It can be easily seen that for any fixed values of $\hat{K}_{II}$ and $\hat{K}_{III}$ we have, when comparing with (24) and (25):

$$\lim_{\tilde{p}_0 \to \pi(1-\nu)} \hat{K}_f \hat{K}_I = \frac{1}{4(1-\nu)} \left(\hat{K}_{IC}^{eff}\right)^2. \tag{26}$$

Finally, we note that for $\hat{K}_{III} = 0$ and $\tilde{p}_0 = 0$ (classical mixed Mode I and II), both normalised stress intensity factors, $\hat{K}_I = \sqrt{1 - \hat{K}_{II}^2}$ and $\hat{K}_f = 0$, are independent of ν.

Eqs. (24) and (25) provide a relationship between the normalised symmetric SIFs, $\hat{K}_I$ and $\hat{K}_f$, and the normalised anti-symmetric SIFs, $\hat{K}_{II}$ and $\hat{K}_{III}$, while also taking into account the influence of the hydraulically induced shear stresses through the pressure parameter $\tilde{p}_0$. This allows for a parametric analysis of the fracture propagation angle, where the independent parameters are $\hat{K}_{II}$, $\hat{K}_{III}$ and $\tilde{p}_0$. This analysis is given in the next section.

3. Determination of the fracture propagation angle

If the crack is only under a Mode I load ($\hat{K}_{II} = \hat{K}_{III} = 0$), it propagates in a self-similar fashion (so that the fracture propagation angle θ_f is equal to zero). However, fractures are often subjected to mixed-mode loadings (Qian & Fatemi, 1996). Therefore, an accurate prediction of the fracture orientation is crucial to defining the path of a crack kink.

In the analysis below, the propagation angle, θ_f, will be determined in the most general case, when all three modes are present. However, when examining the influence of the hydraulically induced shear stress, the analysis will be restricted to the case of mixed Mode I and II ($K_{III} = 0$). In fact, most fractures in geological formations occur under such loading (Li, Xie, Ren, Xie, & Wang, 2013). On the other hand, the applicability of the classical crack redirection criteria raises doubts when accounting for the impact of severe Mode III loading (Lazarus, Buchholz, Fulland, & Wiebesiek, 2008). Recently, an attempt has been made to tackle such cases (Cherny et al., 2017; 2016).

3.1. Maximum circumferential stress (MCS) criterion

The MCS criterion was introduced by Erdogan and Sih (1963). It states that the crack will propagate in the direction where the hoop stress $\sigma_{\theta\theta}$ reaches its maximum over the interval $-\pi < \theta < \pi$:

$$\theta_f = \theta\Big|_{\sigma_{\theta\theta} = \sigma_{\theta\theta}^{\max}}. \tag{27}$$

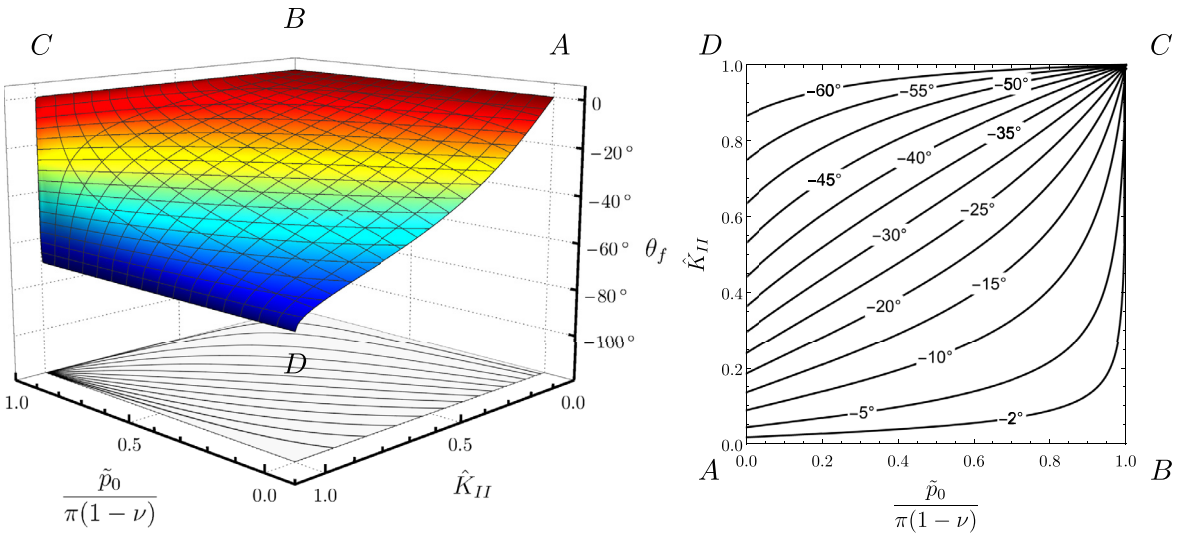

Fig. 3. MCS: Predicted propagation angle θ_f for $\hat{K}_{II} \in [0, 1]$ and $\tilde{p}_0 \in [0, \pi(1-\nu)]$ for $\nu = 0.3$.

Taking (10) into account, we have:

$$\sigma_{\theta\theta}(r,\theta) = \frac{K_{IC}}{\sqrt{2\pi r}}\left[\hat{K}_I \cos^3\frac{\theta}{2} - 3\hat{K}_{II}\sin\frac{\theta}{2}\cos^2\frac{\theta}{2} + 2(1-\nu)\hat{K}_f\cos\frac{3\theta}{2}\right]. \tag{28}$$

According to this formula, the direction of the crack propagation does not depend on the Mode III component or the material toughness K_{IC}. Instead, it hinges on the relationship between the normalised stress intensity factors $\hat{K}_I$, $\hat{K}_{II}$, $\hat{K}_f$ and the Poisson's ratio, ν, if $\hat{K}_f > 0$. It is important to note that there exists only one value of θ_f in the interval $-\pi < \theta < \pi$ that satisfies Eq. (28).

The fracture propagation angle θ_f computed according to the MCS criterion (27) is presented in Fig. 3 for $\nu = 0.3$, and for all admissible values of $\hat{K}_{II} \in [0, 1]$ and $\tilde{p}_0 \in [0, \pi(1-\nu)]$.

The limiting regimes, defined in the parametric space in which the fracture evolves, are denoted by vertices *A*, *B*, *C*, *D* in Fig. 3b.

The value of θ_f in the case of classical linear elastic fracture mechanics ($\tilde{p}_0 = 0$ or edge *AD*) was found analytically (see Erdogan & Sih, 1963):

$$\theta_f = 2\arctan\left(\frac{\hat{K}_I}{4\hat{K}_{II}} - \sqrt{\frac{1}{2} + \frac{\hat{K}_I^2}{16\hat{K}_{II}^2}}\right). \tag{29}$$

On the edge *CD* ($\hat{K}_{II} = 1$), we have from (22) and (24) that $K_{IC}^{eff} = \hat{K}_I = 0$, while the angle θ_f can also be found from (29). This conclusion is, however, not true at the corner C, which also lies on the edge *BC* corresponding to the so-called viscosity dominated regime ($\tilde{p}_0 \to \pi(1-\nu)$, the amount of energy dissipated in the viscous fluid flow is much greater than that released in the brittle fracture). Here, we have $\theta_f = 0$, as the maximum value of the circumferential stress in this case is defined by the third term in (28).

To derive the value of θ_f on the last edge, *AB* ($\hat{K}_{II} = 0$), we must simultaneously maximise the first and the last terms in (28), which holds for $\theta_f = 0$.

We note that in the vicinity of corner *C*, we observe high sensitivity in the angle of crack propagation, θ_f, to changes in the parameters $\tilde{p}_0$ and $\hat{K}_{II}$. In fact, the function $\theta_f(\tilde{p}_0, \hat{K}_{II})$ does not possess a limit at point (1, 1). Indeed, when using the asymptotic estimate (26) and the relationship (22) we have:

$$\hat{K}_f \sim \frac{1-\hat{K}_{II}^2}{4(1-\nu)\hat{K}_I} \quad \text{as} \quad \tilde{p}_0 \to \pi(1-\nu), \tag{30}$$

where both the numerator and the denominator tend to zero as $\tilde{p}_0 \to \pi(1-\nu)$. As a result, the ratio describing the coefficient in the third term in (28) is indeterminate. Therefore, θ_f depends on the load history, and for this reason the limit of expression (30) does not exist at point C. Physically, this phenomenon can be explained by the competition between pure Mode II fracture and the viscosity dominated regime of crack propagation (each of these having different propagation angles).

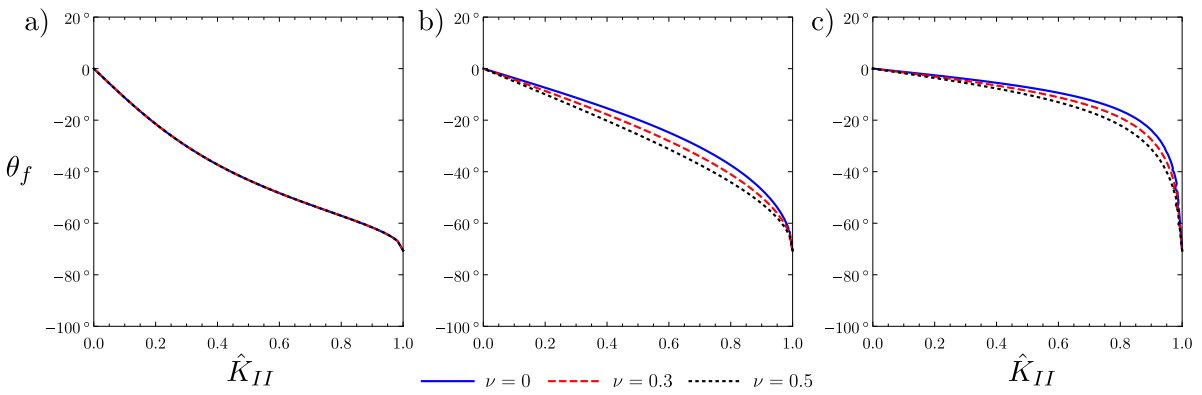

Fig. 4. MCS: Redirection angle, θ_f, for various values of Poisson's ratio and: a) $\frac{\tilde{p}_0}{\pi(1-\nu)} = 0$, b) $\frac{\tilde{p}_0}{\pi(1-\nu)} = 0.5$, c) $\frac{\tilde{p}_0}{\pi(1-\nu)} = 0.9$.

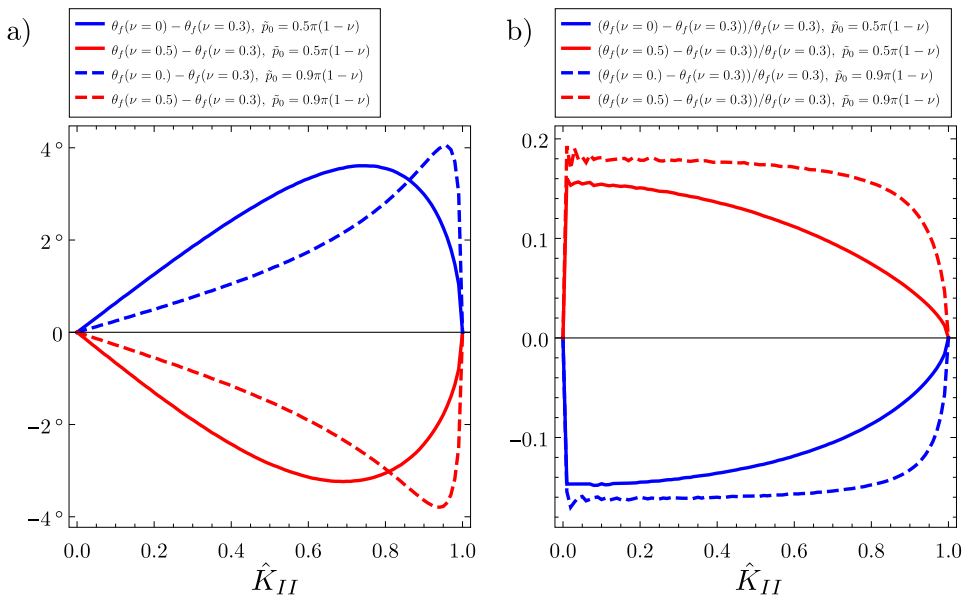

Fig. 5. MCS: Absolute (a) and relative (b) deviations of the redirection angle, θ_f, from a reference value obtained in the case of $\nu = 0.3$ for two limiting values of the Poisson's ratio: $\nu = 0$ and $\nu = 0.5$.

Let us now analyse a possible impact of the Poisson's ratio on the direction of crack propagation (Fig. 4). As expected, for the standard mixed-mode case (without accounting for the singular term induced by the fluid, that is $\tilde{p}_0 = 0,\ \hat{K}_f = 0$), the redirection angle does not depend on the Poisson's ratio ν. This follows immediately from Eq. (28) or (29) and can be seen in Fig. 4a.

In the general case of $\tilde{p}_0 > 0$, the impact of the Poisson's ratio is relatively weak and vanishes when approaching the ends of the interval ($\hat{K}_{II} = 0$ and $\hat{K}_{II} = 1$). As $\tilde{p}_0$ increases, the maximal deviations between respective propagation angles (for various ν) are located closer to the right end of the $\hat{K}_{II}$ interval (see Fig. 5). However, the differences between the redirection angles for various Poisson's ratios are hardly distinguishable, giving maximal deviations between respective results of up to 4° (compare Fig. 5). Thus, according to the MCS criterion, the influence of the Poisson's ratio on crack redirection can be neglected for practical applications, regardless of the fracture propagation regime.

3.2. Minimum strain energy density (MSED) criterion

Another popular fracture propagation criterion is based on the minimum strain energy density (MSED). It was proposed by Liebowitz and Sih (1968) and Sih (1974). For the strain energy density:

$$W = \frac{1}{2}\boldsymbol{\sigma} \cdot \boldsymbol{\varepsilon}, \tag{31}$$

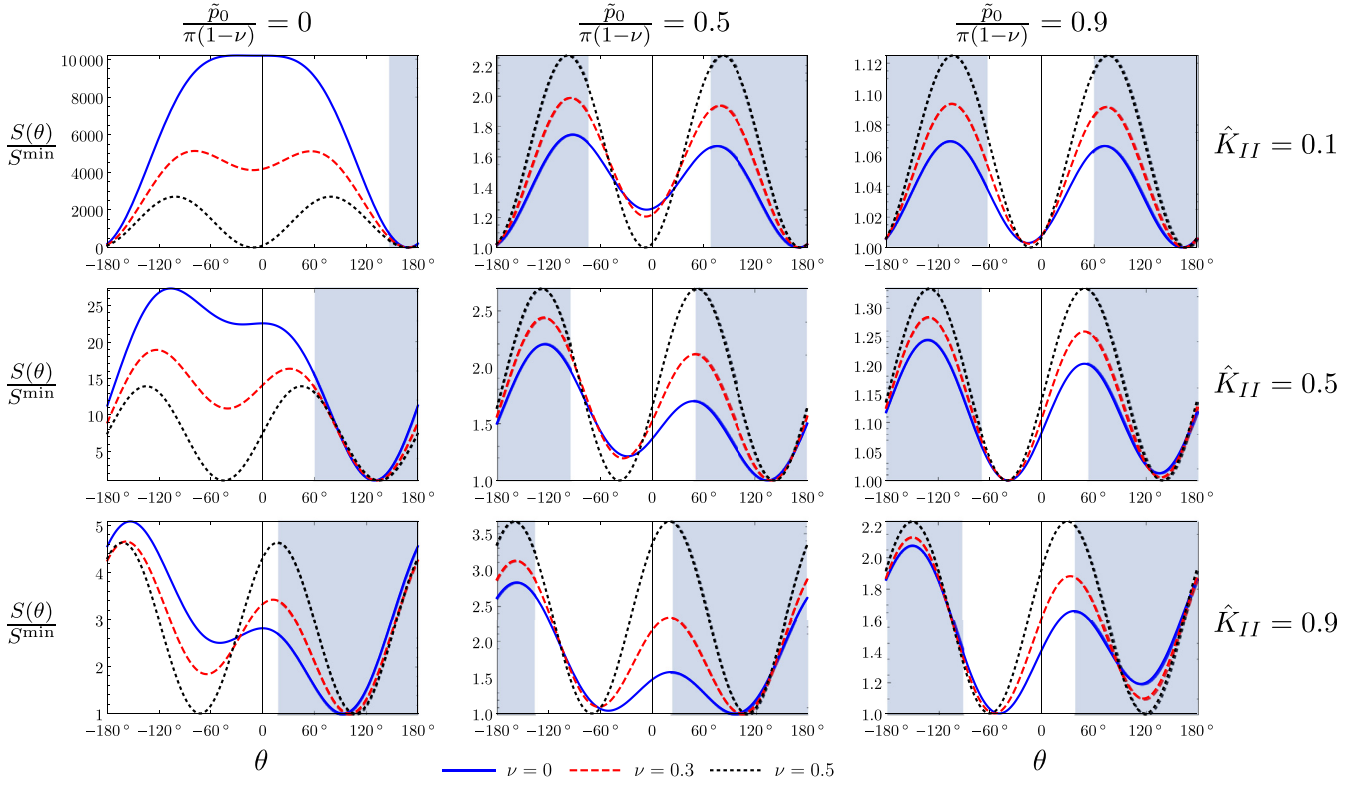

Fig. 6. MSED: Value of $S(\theta)/S^{\min}$ for various values of Poisson's ratio and fixed $\hat{K}_{II}$ and $\tilde{p}_0$. The grey regions on the graphs correspond to the areas where $\sigma_{\theta\theta} < 0$.

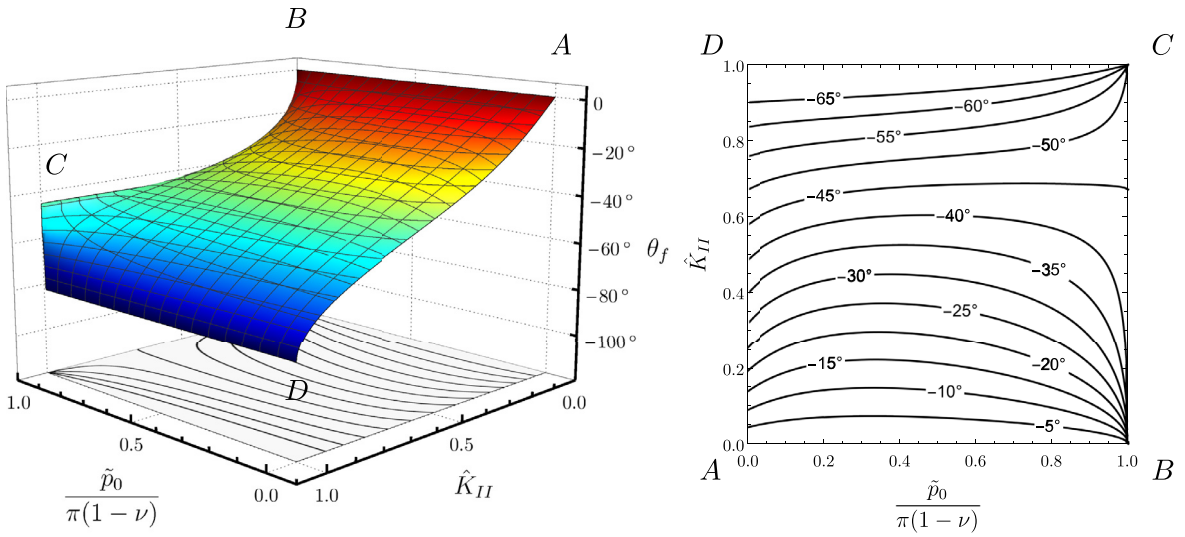

Fig. 7. MSED: Predicted propagation angle θ_f for $\hat{K}_{II} \in [0, 1]$ and $\tilde{p}_0 \in [0, \pi(1-\nu)]$ for $\nu = 0.3$.

it is assumed that the factor $S = Wr$ takes its minimal value in the direction of possible crack propagation:

$$\theta_f = \theta\Big|_{S=S^{\min}}. \tag{32}$$

In the setting of the present paper, the factor S is computed as:

$$S(\theta) = \frac{1+\nu}{2\pi E} K_{IC}^2 \left\{ \frac{\hat{K}_I^2}{2}\cos^2\frac{\theta}{2}[3-4\nu-\cos\theta] + \frac{\hat{K}_{II}^2}{8}[9-8\nu-4(1-2\nu)\cos\theta+3\cos 2\theta] \right.$$
$$\left. + \hat{K}_{III}^2 + 4(1-\nu)^2\hat{K}_f^2 + \hat{K}_I\hat{K}_{II}\sin\theta[2\nu-1+\cos\theta] + (1-\nu)\hat{K}_f\left(2\hat{K}_I\sin^2\theta + \hat{K}_{II}\sin 2\theta\right)\right\}. \tag{33}$$

We note that according to this criterion, and in contrast to MCS, the value of θ_f depends on both the stress intensity factor for Mode III, $\hat{K}_{III}$, and the Poisson's ratio, ν, even in the case of classical LEFM ($\tilde{p}_0 = 0$). However, to remain in the same parametric space in our analysis, the Mode III component will be assumed to be zero.

In Fig. 6 the graphs of $S/S^{\min}$ are plotted for three values of $\nu = \{0, 0.3, 0.5\}$. Each graph refers to a fixed value of $\tilde{p}_0/(\pi(1-\nu)) = \{0, 0.5, 0.9\}$ and a fixed value of $\hat{K}_{II} = \{0.1, 0.5, 0.9\}$.

In each case, it can be seen that there are two local minima (similar behaviour was observed for the classical LEFM by Sih & Macdonald (1974)) that cause ambiguity in identification of the crack redirection angle, that was noticed by Chang (1982). Moreover, in the work of Swedlow (1976) there were indications that, for many combinations of loading modes, the selection of the global minimum of the strain energy density, which in turn corresponds to a global relative maximum of potential energy, leads to incorrect values of the redirection angle. As a result of this analysis, a modification to Sih's statement was proposed that the sought energy minimum does not need to be global. Instead, a local value that corresponds to a positive tensile circumferential stress can be taken:

$$\theta_f = \theta\Big|_{\{S=S^{\min}\}\wedge\{\sigma_{\theta\theta}>0\}}. \tag{34}$$

Furthermore, in the work of Baydoun and Fries (2012), it was suggested that "*the smaller absolute angle is considered as the propagation angle*". We have checked computationally that both assumptions lead to the same result or, in other words, that the minimum of S obtained for the smallest value of θ is also the one that corresponds to $\sigma_{\theta\theta} > 0$. We believe that those assumptions represent a natural choice for the fracture propagation angle according to the MSED criterion.

We now analyse the fracture propagation angle θ_f, as computed in (32), for $\nu = 0.3$ and all admissible values of $\hat{K}_{II} \in [0, 1]$ and $\tilde{p}_0 \in [0, \pi(1-\nu)]$. The corresponding results are presented in Fig. 7.

On the edge AB ($K_{II} = 0$) the angle of crack propagation is $\theta_f = 0$. Furthermore, for pure Mode II ($\hat{K}_{II} = 1$ or edge CD) the solution can be found analytically:

$$\theta_f = -\arctan\frac{2\sqrt{2+\nu-\nu^2}}{1-2\nu}. \tag{35}$$

We recall that for the MCS criterion, the corresponding result was $\theta_f = -2\arctan(1/\sqrt{2})$. However, the biggest difference with MCS appears along the edge *BC* (viscosity dominated regime, $\hat{K}_I = 0$), where the redirection angle was previously equal to zero.

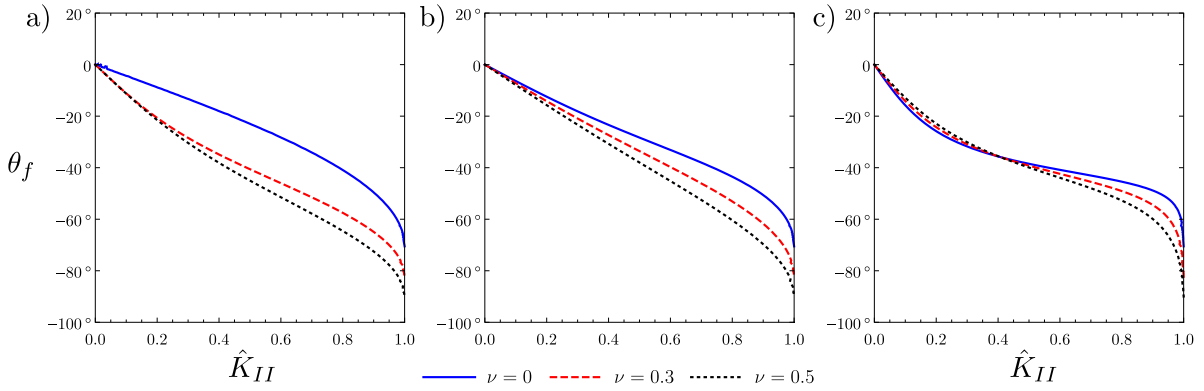

Fig. 8. MSED: Redirection angle, θ_f, for various values of Poisson's ratio and: a) $\frac{\tilde{p}_0}{\pi(1-\nu)} = 0$, b) $\frac{\tilde{p}_0}{\pi(1-\nu)} = 0.5$, c) $\frac{\tilde{p}_0}{\pi(1-\nu)} = 0.9$.

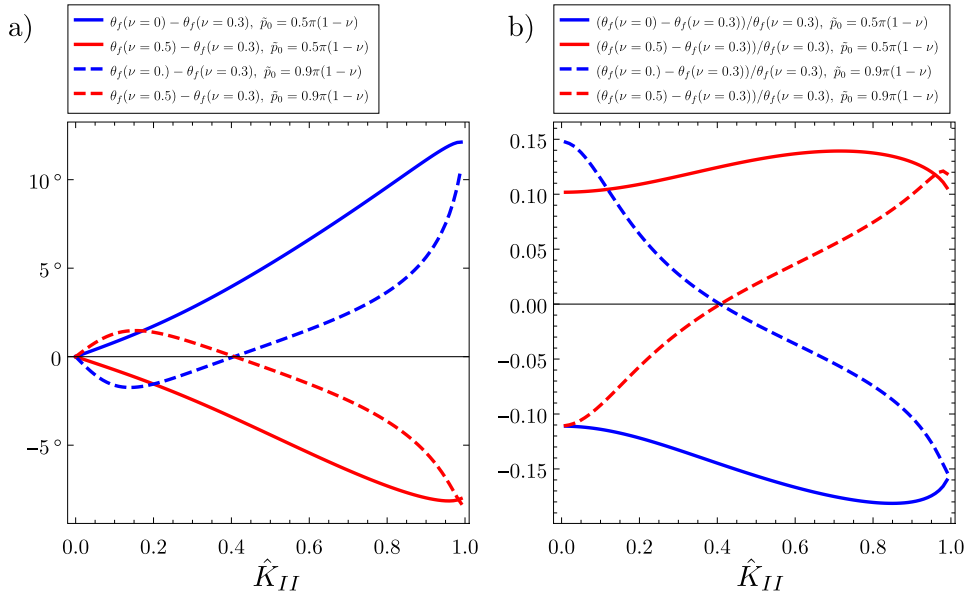

Fig. 9. MSED: Absolute (a) and relative (b) deviations of the redirection angle, θ_f, from a reference value obtained in the case of $\nu = 0.3$ for two limiting values of the Poisson's ratio: $\nu = 0$ and $\nu = 0.5$.

In Fig. 8 – Fig. 9, we show the dependence of θ_f on the Poisson's ratio. The impact of ν is much more pronounced here than in the case of the MCS criterion. The discrepancies between the respective results increase with increasing $\hat{K}_{II}$. Moreover, for $\tilde{p}_0 = 0$, the difference between the angles obtained for $\nu = 0$ and $\nu = 0.5$ is the greatest, amounting to a maximum of 12° (see Fig. 9).

4. Conclusions

In the framework of classical Linear Elastic Fracture Mechanics, the existing criteria for determination of the deflection angle for a small kink give similar results. All of them utilise the asymptotic analysis of the strain-stress fields in the near-tip zone, and the obtained redirection angles usually depend on the relationship between the stress intensity factors (see, for example, the here discussed MSC and MSED criteria for $\tilde{p}_0 = 0$).

We showed that accounting for the hydraulically induced tangential traction on the fracture walls, by introducing one more component of loading, changes the corresponding results with respect to those predicted by the classical criteria. The greatest discrepancies are obtained in the case of substantial external shear load ($\hat{K}_{II} \to 1$), which occurs when the position of the initial crack does not match the orientation of the principal stresses for small material toughness (while approaching the so-called viscosity dominated regime $\tilde{p}_0 \to \pi(1-\nu)$). In such a situation the crack redirection angle is extremely sensitive to the values of both, $\hat{K}_{II}$ and $\tilde{p}_0$.

The criteria analysed in this paper, MCS and MSED, exhibit different sensitivity to the value of Poisson's ratio. Clearly, the predictions made here need to be verified experimentally, which constitutes a real technical challenge.

Finally, other classical criteria for the fracture redirection should be revisited when considering the problem of a fluid driven crack.

Acknowledgments

The authors gratefully acknowledge financial support from the European Union 's Seventh Framework Programme FP7/2007-2013/ under REA Grant agreement numbers: PCIG13-GA-2013-618375-MeMic (A.P.), PITN-GA-2013-606878-CERMAT2 (M.P.) and IRSES-GA-2013-610547-TAMER (M.W.). One of the authors, G. Mishuris, thanks for a support during his visit to Russia by grant 14.Z50.31.0036 awarded to R. E. Alexeev Nizhny Novgorod Technical University by Department of Education and Science of the Russian Federation. Finally, the authors are thankful to Prof. M. Kachanov for fruitful discussions and useful comments.

Appendix A. Functions $\Phi_j(\theta)$ and $\Psi_j(\theta)$ Eqs. (9) and (10)

$$\Phi_I^r(\theta) = \frac{1+\nu}{E}\cos\frac{\theta}{2}[3-4\nu-\cos\theta],$$

$$\Phi_I^\theta(\theta) = -\frac{1+\nu}{E}\sin\frac{\theta}{2}[3-4\nu-\cos\theta],$$

$$\Phi_{II}^r(\theta) = \frac{1-\nu^2}{E}\sin\frac{\theta}{2}\left[\frac{3\nu}{1-\nu}-1+\frac{3\cos\theta}{1-\nu}\right],$$

$$\Phi_{II}^\theta(\theta) = -\frac{1-\nu^2}{E}\cos\frac{\theta}{2}\left[5+\frac{\nu}{1-\nu}-\frac{3\cos\theta}{1-\nu}\right],$$

$$\Phi_{III}^z(\theta) = \frac{4(1+\nu)}{E}\sin\frac{\theta}{2},$$

$$\Phi_\tau^r(\theta) = -\frac{4\left(1-\nu^2\right)}{E}\cos\frac{3\theta}{2}, \quad \Phi_\tau^\theta(\theta) = \frac{4\left(1-\nu^2\right)}{E}\sin\frac{3\theta}{2}.$$

For the plane strain $\Psi^{zz} = \nu\left(\Psi^{rr}+\Psi^{\theta\theta}\right)$.

$$\Psi_I^{rr}(\theta) = \frac{1}{4}\left[5\cos\frac{\theta}{2}-\cos\frac{3\theta}{2}\right], \quad \Psi_I^{\theta\theta}(\theta) = \cos^3\frac{\theta}{2},$$

$$\Psi_I^{r\theta}(\theta) = \frac{1}{2}\cos\frac{\theta}{2}\sin\theta, \quad \Psi_{II}^{rr}(\theta) = -\frac{1}{4}\left[5\sin\frac{\theta}{2}-3\sin\frac{3\theta}{2}\right],$$

$$\Psi_{II}^{\theta\theta}(\theta) = -3\sin\frac{\theta}{2}\cos^2\frac{\theta}{2}, \quad \Psi_{II}^{r\theta}(\theta) = \frac{1}{4}\left[\cos\frac{\theta}{2}+3\cos\frac{3\theta}{2}\right],$$

$$\Psi_{III}^{rz}(\theta) = \sin\frac{\theta}{2}, \quad \Psi_{III}^{\theta z}(\theta) = \cos\frac{\theta}{2},$$

$$\Psi_\tau^{rr}(\theta) = -\Psi_\tau^{\theta\theta}(\theta) = -2(1-\nu)\cos\frac{3\theta}{2}, \quad \Psi_\tau^{r\theta}(\theta) = 2(1-\nu)\sin\frac{3\theta}{2}.$$

References

Adachi, J., Siebrits, E., Peirce, A., & Desroches, J. (2007). Computer simulation of hydraulic fractures. *International Journal of Rock Mechanics and Mining Sciences, 44*, 739–757.

Batchelor, G. (1976). An introduction to fluid mechanics. *Cambridge University Press*. ISBN 978-0-521-09817-5.

Baydoun, M., & Fries, T. P. (2012). Crack propagation criteria in three dimensions using the XFEM and an explicit–implicit crack description. *International Journal of Fracture, 178*, 51–70.

Bunger, A., Detournay, E., & Garagash, D. (2005). Toughness-dominated hydraulic fracture with leak-off. *International Journal of Fracture, 134*(2), 175–190.

Chang, J., Xu, J., & Mutoh, Y. (2006). A general mixed-mode brittle fracture criterion for cracked materials. *Engineering Fracture Mechanics, 73*(9), 1249–1263.

Chang, K. J. (1981). On the maximum strain criterion - a new approach to the angled crack problem. *Engineering Fracture Mechanics, 14*, 107–124.

Chang, K. J. (1982). A further examination on the application of the strain energy density theory to the angled crack problem. *Journal of Applied Mechanics, 49*(2), 377–382.

Cherny, S., Esipov, D., Kuranakov, D., Lapin, V., Chirkov, D., & Astrakova, A. (2017). Prediction of fracture initiation zones on the surface of three-dimensional structure using the surface curvature. *Engineering Fracture Mechanics, 172*, 196–214.

Cherny, S., Lapin, V., Esipov, D., Kuranakov, D., Avdyushenko, A., Lyutov, A., & Karnakov, P. (2016). Simulating fully 3d non-planar evolution of hydraulic fractures. *International Journal of Fracture, 201*, 181–211.

Chudnovsky, A., & Gorelik, M. (1996). Tortuosity of crack path, fracture toughness and scale effect in brittle fracture. In A. Carpinteri (Ed.), *Size-scale effects in the failure mechanisms of materials and structures* (pp. 97–108). London: E&FN Spon.
Cotterell, B., & Rice, J. (1980). Slightly curved or kinked cracks. *International Journal of Fracture, 16*(2), 155–169.
Erdogan, F., & Sih, G. C. (1963). On the crack extension in plates under plane loading and transverse shear. *Journal of Basic Engineering, 85*(4), 519–525.
Garagash, D. (2006). Transient solution for a plane-strain fracture driven by a shear-thinning, power-law fluid. *International Journal for Numerical and Analytical Methods in Geomechanics, 30*, 1439–1475.
Garagash, D., & Detournay, E. (1999). The tip region of a fluid-driven fracture in an elastic medium. *Journal of Applied Mechanics, 67*(1), 183–192.
Goldstein, R. V., & Salganik, R. L. (1974). Brittle fracture of solids with arbitrary cracks. *International Journal of Fracture, 10*(4), 507–523.
Hellen, T. K., & Blackburn, W. S. (1975). The calculation of stress intensity factors for combined tensile and shear loading. *International Journal of Fracture, 11*, 605–617.
Huber, O., Nickel, J., & Kuhn, G. (1993). On the decomposition of the *j*-integral for 3d crack problems. *International Journal of Fracture, 64*, 339–348.
Hussain, M. A., Pu, S. L., & Underwood, J. H. (1974). Strain energy release rate for a crack under combined mode i and mode II. *Fracture analysis ASTM STP, 560*, 2–28.
Irwin, G. (1957). Analysis of stresses and strains near the end of a crack traversing a plate. *Journal of Applied Mechanics, 24*, 361–364.
Lazarus, V., Buchholz, F. G., Fulland, M., & Wiebesiek, J. (2008). Comparison of predictions by mode II or mode III criteria on crack front twisting in three or four point bending experiments. *International Journal of Fracture, 153*(2), 141–151.
Leblond, J. B. (1989). Crack paths in plane situations general form of the expansion of the stress intensity factors. *International Journal of Solids and Structures, 25*(11), 1311–1325.
Li, C. (1989). Vector CTD criterion applied to mixed mode fatigue crack growth. *Fatigue & Fracture of Engineering Materials & Structures, 12*(1), 59–65.
Li, C., Xie, L., Ren, L., Xie, H., & Wang, J. (2013). Evaluating the applicability of fracture criteria to predict the crack evolution path of dolomite based on SCB experiments and FEM. *Mathematical problems in engineering*.
Liebowitz, H., & Sih, G. C. (1968). *Mathematical theories of brittle fracture*. Waltham: Academic Press.
Palaniswamy, K., & Knauss, W. G. (1972). Propagation of a crack under general, in-plane tension. *International Journal of Fracture Mechanics, 8*(1), 114–117.
Paluszny, A., & Zimmerman, R. W. (2017). Modelling of primary fragmentation in block caving mines using a finite-element based fracture mechanics approach. *Geomechanics and Geophysics for Geo-Energy and Geo-Resources, 3*(2), 121–130.
Papadopoulos, G. A. (1988). Crack initiation under biaxial loading. *Engineering Fracture Mechanics, 29*(5), 585–598.
Perkowska, M., Wrobel, M., & Mishuris, G. (2016). Universal hydrofracturing algorithm for shear–thinning fluids: Particle velocity based simulation. *Computers and Geotechnics, 71*, 310–337.
Qian, J., & Fatemi, A. (1996). Mixed mode fatigue crack growth: A literature survey. *Engineering Fracture Mechanics, 55*(6), 969–990.
Rice, J. (1968). A path independent integral and the approximate analysis of strain concentration by notches and cracks. *Journal of Applied Mechanics, 35*(2), 379–386.
Richard, H. A., Fulland, M., & Sander, M. (2004). Theoretical crack path prediction. *Fatigue & Fracture of Engineering Materials & Structures, 28*, 3–12.
Salimzadeh, S., Paluszny, A., & Zimmerman, R. W. (2017). Three-dimensional poroelastic effects during hydraulic fracturing in permeable rocks. *International Journal of Solids and Structures, 108*, 153–163.
Sih, G. C. (1974). Strain-energy-density factor applied to mixed mode crack problems. *International Journal of Fracture, 10*(3), 305–321.
Sih, G. C., & Macdonald, B. (1974). Fracture mechanics applied to engineering problems - strain energy density fracture criterion. *Engineering Fracture Mechanics, 6*, 361–386.
Swedlow, J. L. (1976). Criteria for growth of the angled crack. In *Cracks and fracture, ASTM STP 601, american society for testing and materials* (pp. 506–521).
Theocaris, P. S., & Andrianopoulos, N. P. (1982). The t-criterion applied to ductile fracture. *International Journal of Fracture, 20*, R125-R130.
Williams, J. G., & Ewing, P. D. (1984). Fracture under complex stress - the angled crack problem. *International Journal of Fracture, 26*(4), 346–351.
Williams, M. L. (1957). On the stress distribution at the base of a stationary crack. *Journal of Applied Mechanics, 24*, 109–114.
Wrobel, M., & Mishuris, G. (2015). Hydraulic fracture revisited: Particle velocity based simulation. *International Journal of Engineering Science, 94*, 23–58.
Wrobel, M., Mishuris, G., & Piccolroaz, A. (2017). Energy release rate in hydraulic fracture: Can we neglect an impact of the hydraulically induced shear stress? *International Journal of Engineering Science, 111*, 28–51.
Yehia, N. A. B. (1991). Distortional strain energy density criterion: The y-criterion. *Engineering Fracture Mechanics, 39*(3), 477–485.